Comparison between different photovoltaic solar-assisted heat pumps (PVT-SAHP) configurations with retrofitted photovoltaic panels

ROSSI Cecilia[1], DE ROSA Mattia[2], BIANCO Vincenzo[2,*], SCARPA Federico[2], TAGLIAFICO Luca A.[2]

[1] Acad. of Sciences of the Czech Republic 110 00 Praha

[2]DIME/TEC – Division of Thermal Energy and Environmental Conditioning
University of Genoa
Via All'Opera Pia 15 A, 16145 Genoa
ITALY
*vincenzo.bianco@unige.it

Abstract: - The aim of present study is to investigate different methodologies to retrofit photovoltaic modules (PV), in order to ensure a good cooling effect by adding a thermal plate in the back side of the PV panel to collect heat, thus obtaining a thermal photovoltaic module (PVT). The most promising perspective of this technology is to couple it with a heat pump, in order to obtain a photovoltaic thermal solar-assisted heat pump (PVT-SAHP) system.
This work proposes an investigation of three different solutions to retrofit commercial PV panels. A thermography analyses has been performed in order to verify the cooling effect on the PV module. Results show that retrofitting of existing photovoltaic panels represents an interesting approach in order to employ very simple solutions to increase the overall efficiency of PV system, especially by coupling it with a heat pump.
Finally, in order to study the effective potential of this technology, three different system configurations have been compared in terms of primary energy efficiency, namely a photovoltaic solar assisted heat pump (PVT-SAHP), a solar assisted heat pump (SAHP) and an air-to-water heat pump with a separate set of photovoltaic panels.

Key-Words: Energy System, Heat Pump, Hybrid panel, PV retrofitting, Thermography, PV-SAHP

1 Introduction

A PV/T panel is generally based on the combination of a PV module and a thermal panel (T), permitting to convert simultaneously the solar radiation in both electrical and thermal energy.

The idea of the hybrid panels is based on the observation of a decrease in electrical efficiency of the photovoltaic modules as a consequence of an increase in the modules temperature [1, 2]. This effect is well known and a correlation to determine the panel efficiency as a function of temperature [3] underlines the linear correlation between these two variables.

The simplest way to cool the PV panels, especially in the months when more solar radiation is available, is to couple the PV module with a set of cooling tubes, which allows obtaining two effects: (i) a lower working temperature of the solar cells and, consequently, an increased electrical conversion efficiency, and (ii) the production of thermal energy for heating purposes.

In the last years several of works have been carried out in order to analyze the thermal performance of different PV/T configurations and to develop numerical model for simulating purposes. An exhaustive review on these topics is presented by Charalambous et al. [4]. The research interest was primarily dedicated to the water cooled collectors. A large number of studies have been made: numerical simulations [5], CFD analyses [6], analytical models [7], theoretical [8] and experimental analyses [9,10,11]. In particular, an interesting set of simulations has been done by Ibrahim et al. [12] who evaluated the performance of three different absorber collectors design under various mass flow rates in an optimization perspective. A detailed parametric investigation was also performed by Wu et al. [13] by varying some relevant parameters over a water heat pipe PVT.

Another interesting recent work on hybrid panels was proposed by Yang et al. [14] in which the PV cells are placed on a special substrate of FMG (Functionally Graded Material), composed of an aluminum powder arranged in a matrix of high density polyethylene. The system performance was tested in laboratory with a metal halide lamp, showing an increase of the global efficiency compared with the traditional panels.

Moreover, considering the large energy consumption of energy due to buildings, the development of novel production systems can permit to maximize the energy saving. In particular, the use of renewable sources is mandatory for this purpose (an interesting work regarding the use of the renewable energy in the European Union (EU) has been performed by Popescu and Mastorakis [15]). In this context, several applications based on PV/T have been developed during the last years. As, for instance, Yang et al. [16] studied an interesting application in which a building integrated PV/T system based on a prototype open loop is used to cover the heating load of a domestic house. The study, performed using both numerical and experimental analyses, shows that the thermal efficiency of the system can be improved by 7%.

On the other hand, more complex systems can be realized coupling different energy sources in order to reduce the energy consumption of buildings. In this context, one of the main integrated system developed in the recent years are the solar-assisted heat pumps (SAHP) in which traditional solar collectors are coupled to electrical heat pumps. Generally, different configurations can be adopted: (i) DX-SAHP, in which the refrigerant flows directly inside the PV-modules [17], (ii) an intermediate thermal storage between the heat pump and the solar collectors (ISAHP) [18], and (iii) a geothermal solar-assisted heat pump (GX-SAHP) in which also a ground heat exchanger (GHE) is installed [19]. Moreover, Ibrahim et al. [20] developed recently a solar assisted heat pump system in which thermal evacuated solar collectors are coupled with an heat pump and adopting chemical substance as thermal storage.

Finally, the photovoltaic panels can be used instead of the traditional solar collectors realizing the PV/T solar-assisted heat pump (PV/T-SAHP) system [21]. A review of these system can be found in Oznerger et al. [22]. Generally, this configuration permits to convert the solar irradiation *GA* into electrical power (W_{el}) and in useful heat flow rate for the heat pump (Q_{evap}) increasing the global efficiency of the whole system.

In this context, the object of the present study is to analyze the PV/T-SAHP system realized using retrofitted commercial photovoltaic panel. The retrofitting technique permits to transform existing commercial PV panels in PV/T panel by coupling it with a thermal plate with a water cooled serpentine, without excessive costs. Different approach can be used, depending on the type of type of coupling, the insulation, the serpentine geometries and so on. In order to investigate the behavior of different retrofitting techniques, several experimental tests have been conducted on different prototype at the University of Genoa

In the first part of the present paper, the results obtained during these experimental tests are presented (more details can be found in [23, 24]) as introduction in the following analyses. In particular, a PV-SAHP system is compared with a simple solar assisted heat pump (SAHP) and an air-to-water heat pump with a separate set of photovoltaic panels. The comparison has been performed in terms of primary energy efficiency (COP_{EP}) by using a simplified numerical steady state approach.

2 A brief description of the experimental tests

An extensive experimental analysis is performed on different prototypes of water cooled hybrid panels (W-PVT).

In particular, three different assemblies were obtained by varying the backside and using the frame of the solar panel as a containment structure, as shown in Fig. 1. The first two panels (Fig.1a, b) are arranged with two different types of backside insulation: the prototype a) was insulated with a polyurethane panel, while b) was insulated with a polyurethane foam contained by an aluminum plate at the rear. In the last panel (Fig.1c) simple wood ribs are used to guarantee the contact between the backside of the photovoltaic panel and the thermal aluminum plate. No conductive past or mean is added between the PV panel and the thermal plate.

All the tested hybrid panels are composed of a commercial photovoltaic panel and two water cooled tube-on-plate aluminum panels located at the rear. The main characteristics of the photovoltaic panel are reported in Table 1. In particular, a module efficiency in Standard Test Conditions ($G=1000W/m^2$, light spectrum AM 1.5 and a cell temperature of 25°C) of 13.7% is detected.

The thermal panel presents a tube-on-plate configuration composed of two 1 mm thick aluminum plates and, in each of them, a serpentine is glued with a thermal past. The thermal plate is used to support the two serpentines and to distribute evenly the heat collected by the fluid. To further increase the thermal exchange, the serpentine have an elliptical cross section, ensuring a larger contact surface and, therefore, a better cooling.

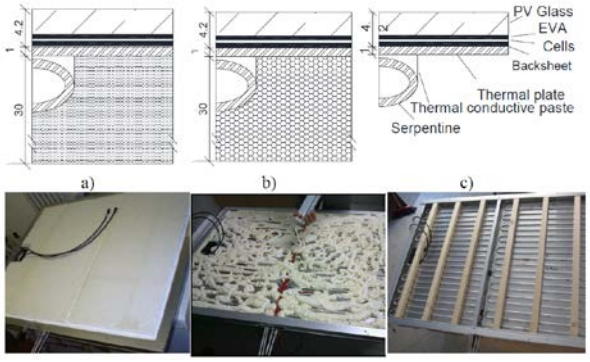

Figure 1: Experimental W-PVT panel insulated using: a) polyurethane panel, b) polyurethane foam, c) hybrid panel without insulation.

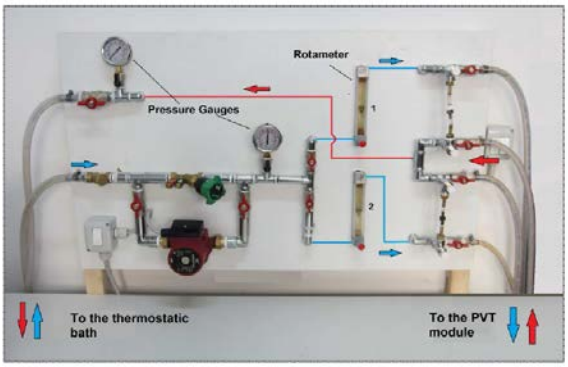

Figure 2: Hydraulic circuit for water distribution

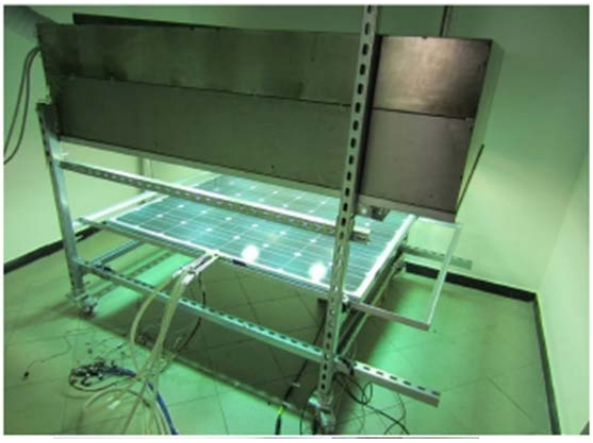

Figure 3: Indoor experimental set-up

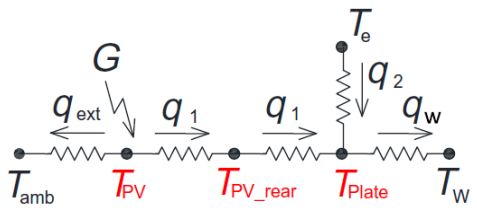

Figure 4: Thermal network of a hybrid panel.

Cells	48 monocrystalline (156.5mm^2) silicon solar cells
Dimensions	1.318x994x46 mm (1.31 m^2)
P_{mpp}	180W_p
V_{oc}	30.0 V
I_{sc}	8.37 A
V_{mpp}	23.7 V
I_{mpp}	7.6 A
η_0	13.7%
NOCT	47.5 °C
α_{Voc}	-104 mV/°C
α_{Isc}	+0.053 %/°C
α_{Pmpp}	-0.485 %/°C

Table 1: Characteristic of the photovoltaic panel adopted for the present work.

The pipe has a circular equivalent external diameter of 8 mm while the equivalent internal diameter is 6 mm. The diameter was chosen in order to minimize the pressure loss, corresponding to a low power consumption of the pumping system and, therefore, an increase in the global primary energy savings. The serpentines were connected to a water distribution system (Fig. 2) with pressure and water flow control and a thermostatic bath for inlet water temperature control.

A set of T-type thermocouples connected to a digital multimeter was used to measure the temperature distribution across the different layers of the hybrid panel. Some thermocouples were placed on the rear side of the photovoltaic panel, in the gap between the photovoltaic panel and the thermal plate, whereas the others were located on the back side of the thermal plate. Finally, inlet and outlet water temperature are also measured by thermocouples.

Several experimental preliminary tests have been performed to evaluate the potential of the proposed hybrid panels. The aim of the experimental tests was to estimate the average global thermal resistance R_t of the W-PVT panel, i.e. the resistance between the external side of the photovoltaic panel T_{PV} and the average water temperature T_W and the thermal resistance $R_{PV\text{-}Al}$ between the backside of the photovoltaic panel T_{PV_rear} and the thermal plate T_{plate} (Fig. 4).

The first tests have been done indoor (Fig. 3) on the prototype a) insulated with the polyurethane (W-PVT(a) panel in Fig. 1. The results of the tests are shown in Table 2. An average thermal resistance of about 0.034m^{2}K/W ± 12% (panel surface 1.31 m^2)

between external surface temperature and mean inlet-outlet water temperatures was measured. An average rear contact resistance between the backside of the photovoltaic panel and the thermal plate of 0.022m^{2}K/W±16% is detected. Considering a thermal air conductivity k_{air}=0.026W/(mK), it corresponds to an air gap of 0.57±0.1mm.

In the same way, the photovoltaic panel W-PVT(b) has been tested in indoor conditions with an irradiation system. The temperature in the different layers of the panel was then measured for various water inlet and ambient temperatures. The results showed a high temperature difference between the backside of the photovoltaic and the backside of the aluminum plate (Table 3). In these working conditions, an average thermal resistance of about 0.108m^{2}K/W±5% between external surface temperature and mean inlet-outlet water temperatures has been calculated.

Moreover, an average rear contact resistance between the backside of the photovoltaic panel and the thermal plate of 0.079 m^{2}K/W ± 5.5%, corresponding to an air gap of 2.05±0.11mm, was estimated. The presence of an air gap was due to a poor foam expansion and a consequent separation of the aluminum plate from the photovoltaic panel. Therefore, it is evident that the use of foam is not recommended for existing PV retrofitting.

Finally, the photovoltaic panel W-PVT(c), assembled with wooden ribs in order to improve the adhesion between the two panels without insulation, was tested both indoor and outdoor. Fig. 5 shows the comparison between the W-PVT(c) and the traditional PV panel in terms of temperature profiles during the outdoor test in comparison.

Moreover, Table 4 reports the results of both outdoor and indoor test. The thermal resistance between external surface temperature and mean inlet-outlet water temperatures is equal to 0.030m^{2}K/W±8%, while an average rear contact resistance between the backside of the photovoltaic panel and the thermal plate of 0.017m^{2}K/W±9% is obtained corresponding to an air gap of 0.45±0.04mm.

The presence of air greatly highlighted in the previous analyses for the insulated prototype (W-PVT(a,b)) affects the thermal resistance (and, therefore, the heat transfer coefficient) between the solar cells and the thermal absorber, reducing the cooling of photovoltaic panel and, consequently, the electrical efficiency. Moreover, if the air thickness is not uniform, the PV temperature distribution along the panel surface can show significant difference.

T_{w_in} [°C]	T_{w_out} [°C]	T_w [°C]	$Q_3=Q_w$ [W/m^2]	$T_{plate-rear}$ [°C]	$T_{PV-rear}$ [°C]	T_{PV} [°C]	R_t [m^{2}K/W]	R_{PV-Al} [m^{2}K/W]	S_{PV-Al} [mm]
44.8	43.0	43.9	-136.5	42.4	38.9	39.2	0.034	0.026	0.66
10.7	12.1	11.4	114.5	11.4	13.5	15.1	0.032	0.019	0.49
5.6	7.0	6.3	111.7	6.6	9.0	10.3	0.036	0.021	0.54
							0.034	**0.022**	**0.57**

Table 2: Indoor test on the hybrid panel W-PVT(a). The measures are referred to the average values of the measuring points and interest more than 80% of the panel surface.

G W/m^2	T_{amb} °C	T_{w_in} °C	T_{w_out} °C	T_w °C	$Q_3=Q_w$ W/m^2	$T_{plate-rear}$ °C	$T_{PV-rear}$ °C	T_{PV} °C
≈400 (12lamps)	20	14.2	17.3	15.7	246.5	22.3	39.5	40.74
≈400 (12lamps)	20	24.5	26.7	25.6	174.0	30.1	47.1	47.93
≈400 (12lamps)	30	24.7	27.8	26.2	241.9	32.0	51.8	53.03
≈400 (12lamps)	30	12.7	17.5	15.1	385.3	23.0	48.4	50.34

Table 3: Indoor test on the hybrid panel W-PVT(b). The measurements are referred to the average values of the measuring points.

G W/m^2	T_{amb} °C	T_{w_in} °C	T_{w_out} °C	T_w °C	$Q_3=Q_w$ W/m^2	Q_1 W/m^2	$T_{plate-rear}$ °C	$T_{PV-rear}$ °C	T_{PV} °C
≈400 (12lamps)	21.5	14.4	20.0	17.2	447	403	21.1	28.8	29.7
≈200 (6lamps)	20.8	14.2	17.4	15.8	249	199	18.4	21.8	22.0
890	15.7	14.0	20.2	17.1	491	506	23.9	33.5	35.3

Table 4: Indoor and outdoor test results on the W-PVT(c).

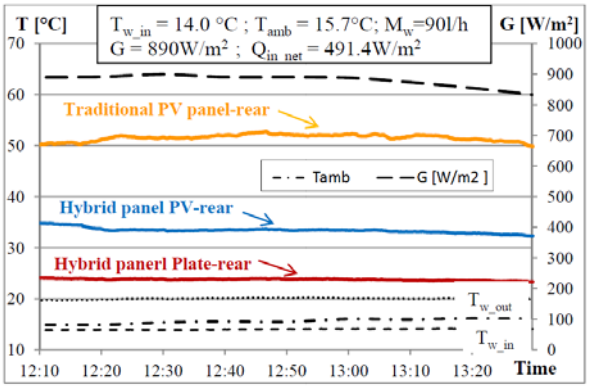

Figure 5: Temperature distribution for W-PVT(c) prototype in comparison with a traditional PV panel in quasi steady state operation during outdoor test.

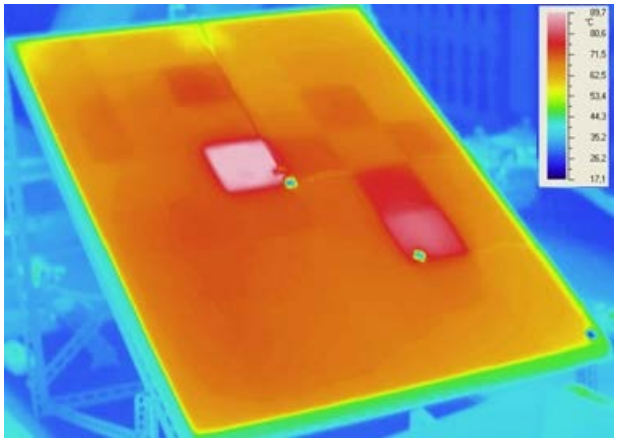

Figure 6: Thermal imaging of the W-PVT panel (a) during the heating indoor tests

In order to verify the cooling effect, a thermography analyses has been conducted on the prototype W-PVT(a) and W-PVT(c), which are compared with the traditional PV module.

Fig. 6 shows a thermal imaging of the prototype W-PVT(a), and highlights that the thermal contact between the photovoltaic and thermal panels is not uniform, in fact some warmer zone are detected, highlighting the presence of a high resistance between the panel and the serpentine. This causes a decrease of the electric conversion efficiency, therefore it is necessary to limit this effect.

A thermal imaging of the photovoltaic panel and the hybrid panel W-PVT(c) during the outdoor tests (Fig. 7) highlights the presence of a hotter area in the middle of the panel as seen during the heating test of the panel W-PVT (a) (Fig. 6). The presence of this small area (around 4% of the total surface) in the same position even for this configuration is probably due to a small overlap of the thermal plates as a consequence of a non-flat area. This issue could be easily overcome by using new thermal plates. Even with the presence of this hotter area, the hybrid panel appears to be clearly colder. The average temperature difference is around 10°C, corresponding to an increase in electrical efficiency of about 5%. The presence of area of non-adherence could be also settled by using some thermal conductive paste.

Finally, it is possible to conclude that the prototype a) and c) appears the best solution.

3 PV-SAHP system performances

The growing interest on this technology is proven by the increasing share of PVT-SAHP papers over the total published PVT studies in the last years.

Generally, the simpler application consists in combining a PVT collector to a direct expansion solar assisted heat pump (Fig. 8b): the refrigerant fluid flows directly within a channel on the backside of the panel. The heat is extracted in the evaporator, the temperature and the pressure are increased at the compressor, and the heat is released at the condenser before the refrigerant flows through the expansion valve or through a capillary to start again the cycle. The solar irradiation *GA*, is converted by the photovoltaic evaporator into electrical power (W_{el}) and in useful heat flow rate for the heat pump (Q_{evap}). A part of the solar irradiation can be also wasted (Q_{loss}) because of convection and radiation losses between the panel and the ambient air.

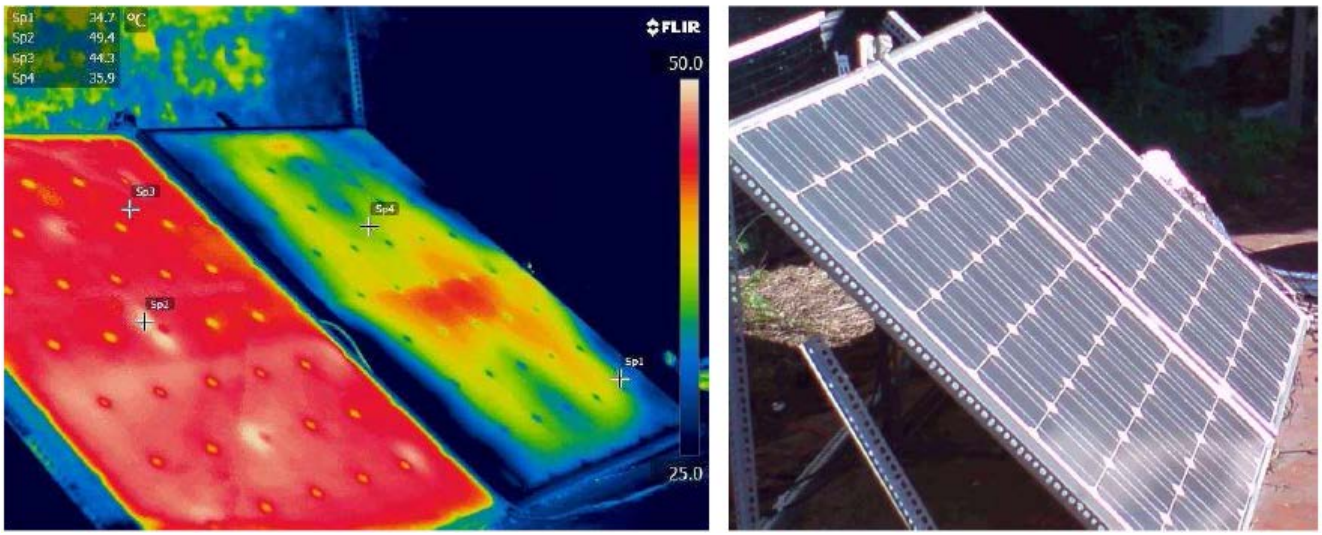

Figure 7: Thermal imaging of the W-PVT panel (c) during the external tests

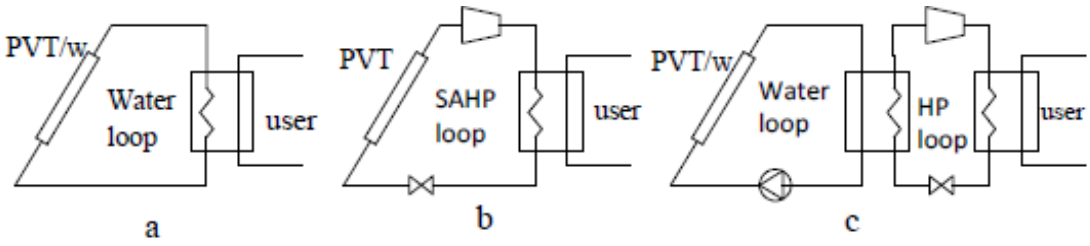

Figure 8: Possible embodiments of PVT-SAHP configurations: a) simple PVT/w water loop; b) direct expansion PVT-SAHP heat pump assembly; c) PVT/w-SAHP configuration: PVT/w water loop coupled to water to water heat pump loop

The energy balance on the hybrid panel can be expressed as follows:

$$\alpha GA = W_{el} + Q_{evap} + Q_{loss} \quad (2)$$

where α is the absorption coefficient of the hybrid panel surface in the solar wavelength spectrum, and varies between 0.5 and 0.9. The heat transfer rate from the panel to the ambient air could be expressed by the usual linearized equation:

$$Q_{loss} = KA(T_{PV} - T_{amb}) \quad (3)$$

where K is the overall (convective and radiative) heat transfer coefficient between the panel and the ambient, assumed in the range K = 5 ÷ 10 W/m^{2}K for traditional insulated panels and up to 15 ÷ 25 W/m^{2}K in photovoltaic unglazed panels.

The heat absorbed by the heat pump (Q_{evap}) is converted at the condenser in useful heat for the user (Q_c) together with the compressor power (W_c) for the following heat pump energy balance:

$$Q_c = Q_{evap} + W_c \quad (4)$$

Another configuration consists in separating the refrigerant loop with the solar collector from the storage tank, thus realizing an indirect solar-assisted heat pump (Fig. 8c). In this configuration, a water loop extracts heat from the PV collectors, while the storage tank has the function of evaporator.

Generally, the standard Coefficient of Performance (COP) permits to evaluate the global performance of standard heat pump systems and is defined as shown in Eq. 5:

$$COP = \frac{Q_c}{W_c} = 1 + \frac{Q_{evap}}{W_c} \quad (5)$$

However the COP represents only the ratio between the heat produced at the condenser and the power absorbed by the compressor and it is not suitable to estimate the PVT-SAPH performance as it does not consider the electrical production of the PV modules. For this reason, Ji et al. [25] proposed an overall performance parameter for these systems, defined as follows:

$$COP_{PVT} = \frac{Q_c + \frac{W_{el}}{\eta_{power}}}{W_c} \quad (5)$$

where η_{power} represents the average electricity primary energy conversion of electrical production.

Nevertheless the parameter proposed in literature to evaluate and compare the performance of the PVT-SAHPs is suitable only to make a comparison between different types of PVT-SAHPs, whereas it would be interesting to compare the PVT-SAHP with other energy sources or, for example, with traditional heat pumps.

In the present work a new efficiency parameter in terms of primary energy is introduced (Eq. 6).

$$COP_{EP} = \frac{\frac{Q_c}{\eta_{burn}} + \frac{W_{el}}{\eta_{power}}}{\frac{W_c + W_{pump}}{\eta_{power}}} \quad (6)$$

where η_{power} is the average electricity-primary energy conversion factor and η_{burn} is the average heat-primary energy conversion factor.

In order to understand the behavior and the potential of the PVT-SAHPs, the experimental work performed by Ji et al. [25] has been selected and analyzed in terms of COP and COP_{EP}.

The experiments were performed in Hefei (Central China) for 4 days in November under similar weather conditions with different condenser supply water temperature (20°C; 30°C; 40°C; 50°C). To understand the behavior and to analyze the performance of the system we refer only to the maximum and the minimum water condenser temperature. For 20°C and 50°C the trends of the different COP during the day are shown in Fig. 9a. As expected the COP is higher than the COP_{EP}, and all the performance parameters follow the trend of the solar radiation. The variation of the COP_{EP} against the solar radiation G has shown in Fig. 9b. Generally, for the same solar radiation the COP_{EP} is

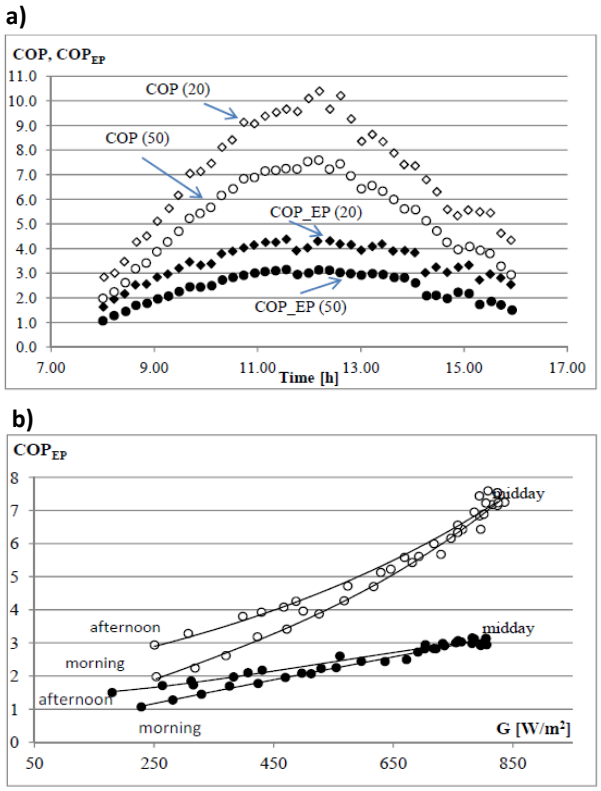

Figure 9: Variation of COP and COP_{pvt_EP} for 20°C and 50°C inlet temperature at the condenser a) during the day and b) as function of G. The data are taken from Ji et al. 2008 [25]

higher in the afternoon when the ambient temperature is higher. The experimental data confirm the importance of the ambient temperature on the performance of the PVT-SAHP.

To have an idea of the potential of this technology, a preliminary comparison between the PVT-SAHP and the traditional heat pump could be achieved. The average coefficient of performance of a water to water heat pump is around 4-4.5 for T_{evap} = 10°C and the water inlet temperature T_{w_in}= 40°C, while the average COP of an air to water heat pump is 3 ÷ 3.3, when the heat pump works between 6°C and 40°C. The corresponding COP in terms of primary energy are, respectively, 1.8÷2.0 and 1.4÷1.5. These values are compared to the COP_{EP} obtained from the experimental data provided by Ji et al. [25].

The average COP_{EP} for a water condenser supply temperature of 40°C and an ambient temperature of 15°C is 3.2. Moreover, the average power consumption is considered assuming a value of 1.9kW for a 40°C water condenser temperature. The results are shown in Table 5, where it is possible to note the advantage of the PVT-SAHP systems, especially in terms of primary energy savings.

	COP	COP_{EP}
Water to water heat pump	4.1	1.9
PVT-SAHP	4.4	2.9

Table 5: Performance comparison between a water-to-water heat pump and a PVT-SAHP (data extracted from Ji et al. [10]).

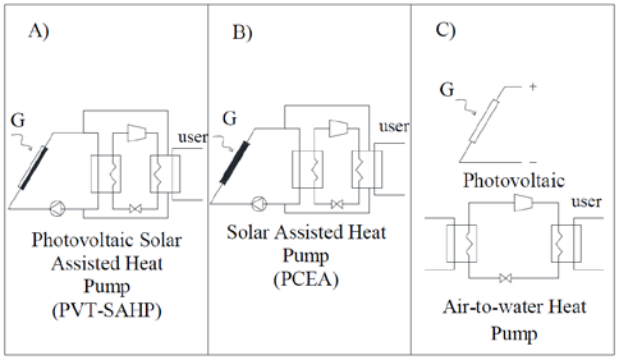

Figure 10: Schematic diagram of the three different plant configuration investigated in the present work.

In order to investigate the real potential of this technology, three different configurations are compared:

- configuration A: a photovoltaic solar assisted heat pump PVT-SAHP (hybrid panel coupled to a traditional water-to-water heat pump);
- configuration B: a simple solar assisted heat pump PCEA (thermal panel coupled to a traditional water-to-water heat pump).
- configuration C: an air-to-water heat pump and a set of photovoltaic panels (same area of the panels used in the other configurations).

The solar assisted heat pumps are both connected to the same commercial water-to-water heat pump, chosen in order to satisfy a given user heat load and the electrical output is considered as an added value for the user. The diagrams of the different configurations are shown in Fig.10.

The comparison was done for three different locations, characterized by different number of degree days (Palermo: HDD=751; Genoa: HDD=1435; Turin: HDD=2617), supposing a nominal heat rate of 100kW, corresponding approximately to a monthly averaged heat user load of 35000kWh/month.

The water was provided to the users at 50°C, with a 15°C network water. In terms of DHW, the daily requirement of the user is 28160 liters. The

monthly average ambient temperature and solar radiation of the three cities were considered.

The comparison was done in terms of the primary energy coefficient of performance defined as the ratio between the primary energy generated and consumed, adapted for this case study (Eq. 7).

$$COP_{EP} = \frac{\frac{Q_p}{\eta_{burn}} + \frac{W_{el}}{\eta_{power}}}{\frac{W_c + W_{pump}}{\eta_{power}} + \frac{Q_{int}}{\eta_{burn}}} \quad (7)$$

where Q_p represents the heat given to the user (100kW), W_{el} the electrical power produced by the photovoltaic cells (if any), W_c the power consumed by the compressor of the heat pump, W_{pump} the power used by the circulation pump to pump the fluid inside the panel (if any) and Q_{int} represent the integration heat, if necessary.

The total output power W_{el} of the PV panel field is calculated from the single panel production considering a Balance of System (BOS) of 0.85, in order to correctly estimate the productivity of the photovoltaic panel. The operating limits of the commercial heat pump related to the water temperature at the evaporator outlet are a minimum temperature of 4°C and maximum 18°C.

The panels in the solar assisted heat pumps works as an indirect evaporator (see Fig. 11). No particular problems are expected on the condenser side, since a fixed 50°C operating temperature is assumed. To avoid freezing problems, a water-glycol mixture was circulated under the panels (specific heat C_p=3800J/kg/K) and the panel temperature was kept above 5°C to avoid ice over the panel, in accordance with the operating limits of the heat pump.

When the environmental conditions are unfavorable (i.e. in winter), the heat pumps works at 5°C and the user demand is reached by means of a boiler integration. When the solar radiation and the

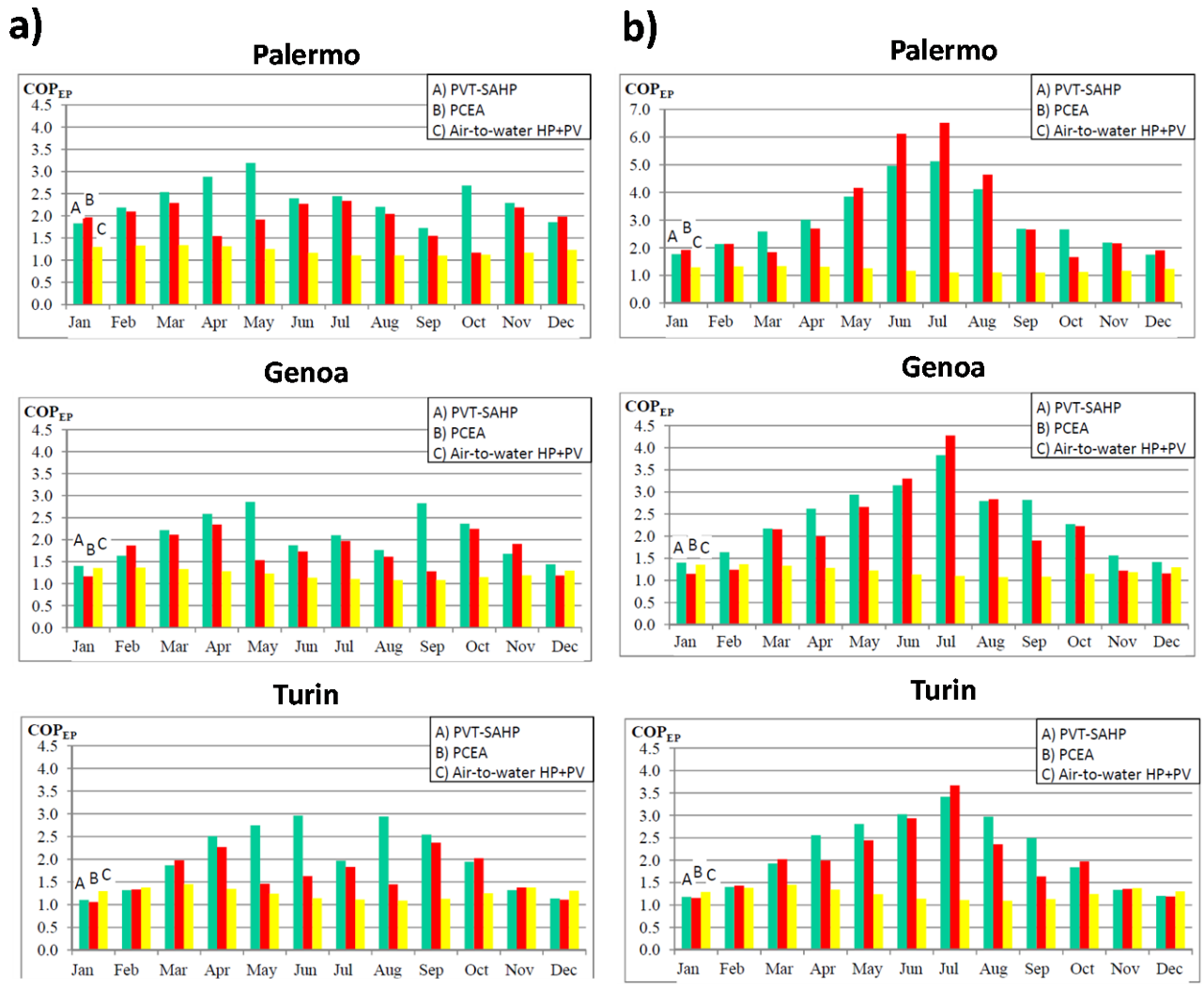

Figure 11: Comparison between the three configurations in terms of COP_{EP} for a) not insulated and b) insulated panels, in different Italian localities with an h_{ca} = 65 W/(m^{2}K).

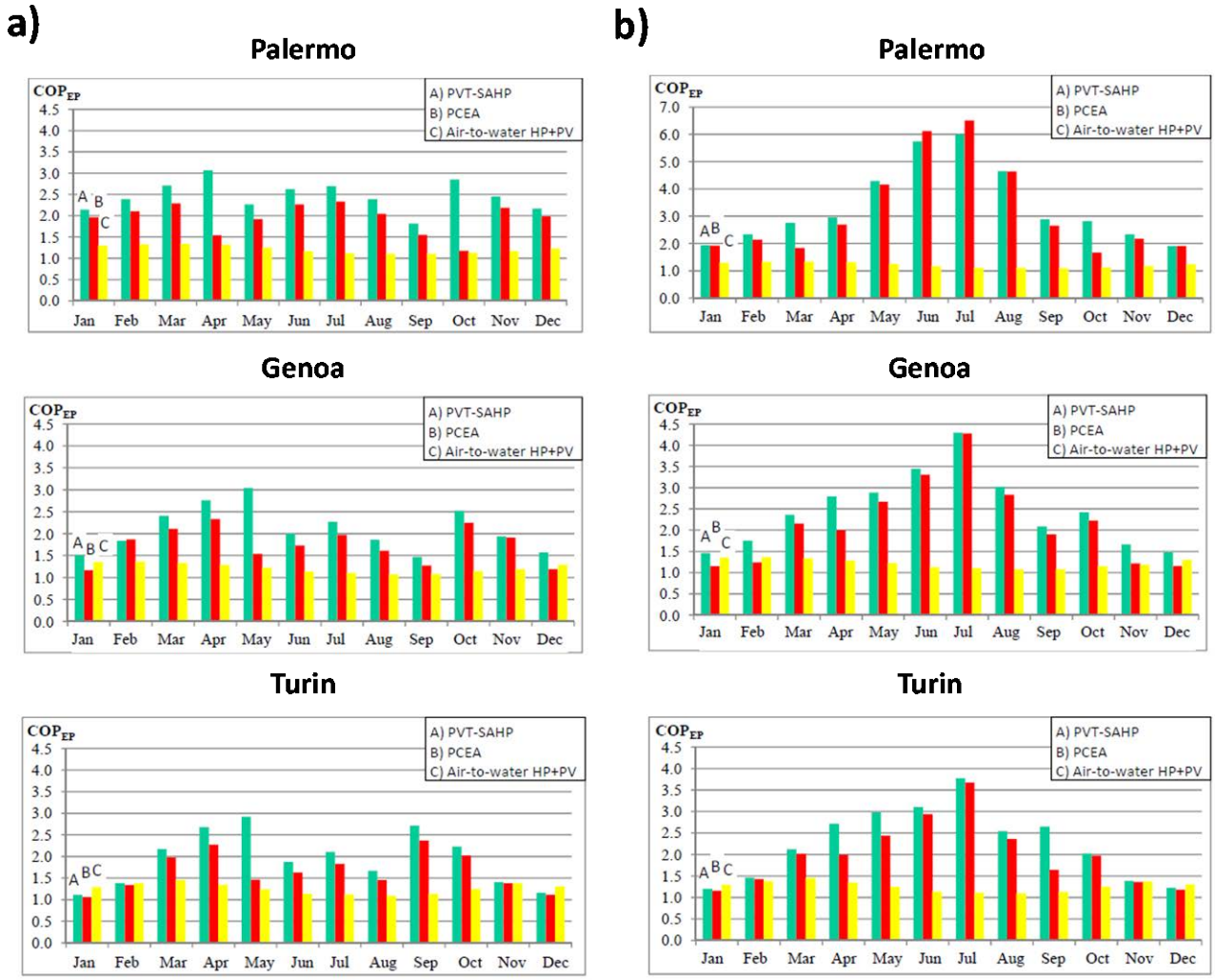

Figure 12: Comparison between the three configurations in terms of COP_{EP} for a) not insulated and b) insulated panels, in different Italian localities with an h_{ca} = 500 W/(m^2K).

ambient temperature are high enough, the system bypass the heat pump and the user demand is satisfied only by the panel and a small boiler integration. The panel disconnected from the heat pump is modeled through the f-chart method [26] for solar liquid panels. Finally, the configurations have been analyzed considering both a not insulated and an insulated (δ_{INS}=30mm, k_{INS}=0.03W/mK) panel.

The results are shown in Fig. 11-12 where the monthly variation of the COP_{EP} are presented for each configuration and for two different values of h_{ca} (Fig. 11: h_{ca} = 65 W/m^2K; Fig. 12: h_{ca} = 500 W/m^2K). The average COP_{EP} for each location and each plant configuration are summarized in Table 6. Moreover, Table 6 shows the average COP_{EP} for each location and each plant configuration.

The average primary energy coefficient of performance is clearly higher when a solar assisted heat pump (PVT-SAHP or PCEA) is used, compared to the plant configuration with the air-to-water heat pump and photovoltaic panels. From the observation of the solar assisted heat pump plant configurations, it is possible to note that the COP_{EP} is higher for the insulated panels. This difference is related to the different behavior of the plant when the heat pump is bypassed and only the thermal or hybrid panels are used (see also as an example from May to September in Fig. 11b - Palermo).

If the insulated panels are used the water temperature increase, due to lower thermal losses, and therefore the fraction of the monthly heat demand satisfied by the sun is much larger and the heat integration is much lower. The increase in the

	Palermo		Genoa		Turin	
	Insulated	Not insulated	Insulated	Not insulated	Insulated	Not insulated
Configuration A65	3.1	2.4	2.4	2.1	2.2	2.0
Configuration A500	3.4	2.5	2.5	2.1	2.3	1.9
Configuration B	3.2	1.9	2.2	1.7	2.0	1.7
Configuration C	1.2	1.2	1.2	1.2	1.3	1.3

Table 6: Average COP_{EP} for each location and each plant configuration. A65: PVT-SAHP with h_{ca} = 65 W/m^{2}K; A500: PVT-SAHP with h_{ca} = 500 W/m^{2}K; B) PCEA and C) the air-to-water heat pump and PV panels. The average COP_{EP} is calculated both for a not insulated and an insulated (δ_{INS}=30mm, k_{INS}=0.03W/mK) panel.

water temperature involves a decrease in the electrical efficiency and electrical power output for the PVT-SAHP, however this decrease is really small compared to the decrease in heat integration thus resulting in an increase in the primary energy COP.

The PVT-SAHPs are always advantageous in terms of primary energy compared to the traditional solar thermal assisted heat pumps (SAHP). The only case where the traditional solar assisted heat pump (configuration B) is convenient compared to the photovoltaic solar assisted heat pump is for the insulated panel configuration in Palermo (see Tab. 6 and Figure 11b). In this case the average primary energy coefficient of performance is higher because it increases considerably in summer, when the heat pump is bypassed and only the panels are used.

At this time the thermal insulated panel can satisfy around 85%-90% of the monthly heat demand, thus implying a low heat integration, compared to the 75%-80% satisfied by the hybrid panel without thermal paste. Only in this case, due to the really low heat integration the advantage of electrical power produced by the hybrid panel is completely negligible, otherwise the PVT-SAHP appears to be the best solution. The use of a thin layer of thermal paste (configuration A500), increases the primary energy coefficient of performance, compared to a simple hybrid panel (configuration A65). Also in this case there is an exception represented by the not insulated panel in Turin (see table Table 6 and compare Figure 11.b and Figure 12b). This effect is also partly noticeable for the not insulated panel in Genoa (see table Table 6 and compare Figure 11a and Figure 12a). The use of thermal paste leads, in fact, to a higher water temperature and a lower panel temperature due to a better heat transmission. This implies that the heat pump is bypassed more frequently, as the water temperature reach the working limit of the heat pump. In the case of Torino when the heat pump is bypassed, due to the low solar radiation and the absence of thermal insulation, a great heat integration is required (the panel itself is able to satisfy only 30%-40% of the heat demand).

4 Conclusion

The present paper reports a study about water cooled retrofitted solar hybrid panels achieved by means of experimental tests. In the first part of the paper, three different backside insulations applied to three PV commercial modules with the same characteristics are proposed and experimentally analyzed.

The results show that the use of a polyurethane foam in order to fix the thermal plate to the PV module does not represent a good retrofitting solution, showing the presence of an air gap due to a poor foam expansion and a consequent separation of the aluminum plate from the photovoltaic panel.

Moreover, in order to verify the cooling effect on the PV module several thermography analyses have been conducted, limited to prototype W-PVT(a) and W-PVT(c). In particular, the thermal imaging of the prototype W-PVT(a) shows that the thermal contact between the photovoltaic and thermal panels is not uniform along the whole panel surface, causing a substantial temperature difference which affects the thermal and electrical performance of the prototype. The hybrid panel W-PVT(c) during the outdoor tests highlights the presence of a small hotter area (about 4% of the total surface) in the middle of the panel as seen during the heating test of the panel W-PVT (a),

probably due to a small overlap of the thermal plates. As a conclusion, it is possible to state that the wood ribs configuration permits the best performances guaranteeing a most effective contact between the thermal plate and the PV module.

The second part of the paper compares three different configurations in terms of primary energy COP. In particular, A new primary energy coefficient of performance was introduced to make a consistent comparison among different technologies (solar, heat pumps, solar assisted heat pumps) for the same thermal load and available surface.

In particular, the main advantage obtained by coupling a hybrid panel to a heat pump is the possibility of keeping the temperature of the panel lower than ambient temperature, thus increasing the global efficiency of the panel while providing hot water to the user, showing an average primary energy coefficient of performance around 2.5 – 3.0 for the photovoltaic solar assisted heat pump and 1.2 – 1.4 for an air-to-water heat pump in the same working conditions.

The results also highlight that the presence of an insulation on the backside of the thermal panel, often found in the commercial hybrid panels, is not really advantageous. Indeed if no refrigeration is provided, the presence of insulation determine an increase in the panel temperature and a consequent decrease in the electrical efficiency of the photovoltaic cells. The insulation represents also a disadvantages if the panel temperature is kept below the ambient temperature, since the heat collected is lower.

The comparison between different plant configurations in three different Italian locations (Palerno, Genoa, Turin) was performed in terms of primary energy coefficient of performance COP_{EP}, which is defined and described in chapter 5.3. The comparison shows that the efficiency of the photovoltaic solar assisted heat pumps is much higher than the efficiency of the traditional air-to-water and water-to-water heat pumps. In particular, for the same user heat load, the average value of this parameter is around 1.2 for the air-to-water heat pumps, 1.5 for the water-to-water heat pumps and around 2.8 for the photovoltaic solar assisted heat pumps.

References:

[1] Skoplaki E, Palyvos JA. On the temperature dependence of photovoltaic module electrical performance. *Solar Energy*, Vol.83, No.5, 2009, pp. 614-624.

[2] Skoplaki E, Palyvos JA. Operating temperature dependence of photovoltaic module: A survey of pertinent correlations. *Renewable Energy*, Vol. 34, No. 1, 2009, pp. 23-29.

[3] Evans DL, Simplified method for predicting photovoltaic array output, *Solar Energy*, Vol.27, No.6, 1981, pp. 555-560.

[4] Charalambous PG, Maidment GG, Kalogirou SA, Yiakoumetti K. Photovoltaic thermal (PV/T) collectors: A review. *Applied Thermal Engineering*, Vol 27, 2007, pp. 275-286.

[5] Zondag HA, de Vries DW, van Helden WGJ, , van Steenhoven AA, van Zoligen RJC. The thermal and electrical yield of a PV-thermal collector. *Solar Energy*, Vol.72, No.2, 2002, pp. 113-128.

[6] Ibrahim A., Othman MY, Ruslan MH, Alghoul MA, Yahya M, Zaharim A, Sopian K. Performance of photovoltaic thermal solar collector (PV-T) with different absorber design. *WSEAS Tranactions on Environment and Development*, Vol.5, No.3, 2009, pp.321-330.

[7] Sandnes B, Rekstad J. A photovoltaic/thermal (PV/T) collector with a polymer absorber plate: experimental study and analytical model. *Solar Energy*, Vol.72, No.1, 2002, pp. 63-73.

[8] Vokas G, Christandonis N, Skittides F. Hybrid photovoltaic-thermal system for domestic heating and cooling – A theoretical approach. *Solar Energy*, Vol. 80, No.5, 2006, pp. 607-615.

[9] Tripanagnostopoulos Y, Nousia T, Souliotis M, Yianoulis P. Hybrid photovoltaic/thermal solar energy systems. *Solar Energy*, Vol. 72, No.3, 2002, pp. 217-234.

[10] Tripanagnostopoulos Y. Aspects and improvements of hybris photovoltaic/thermal solar energy systems. *Solar Energy*, Vol. 81, No.9, 2007, pp. 11171131.

[11] Saitoh H, Hamada Y, Kubota H, Nakamura M, Ochifuji K, Yokoyama S., et al. Field experiments and analysis of a hybrid solar collector. *Applied Thermal Engineering*, Vol.23, No.16, 2003, pp.2089-2105.

[12] Ibrahim A, Daghigh R, Jin GL, Salleh MHM, Othman MH, Ruslan MH, Mat S, Ibrahim K, Zaharim A, Sopian K. Thermal theoretical study on PVT water based collectors. In *Proceedings of the 2010 American conference on Applied mathematics.*

[13] Wu SY, Zhang QL, Xiao L, Guo FH. A heat pipe photovoltaic/thermal (PVT) hybrid system and its performance evaluation. *Energy and Buildings*, Vol.43, No.12, 2011, pp. 3558–3567.

[14] Yang DJ, Yuan ZF, Lee PH, Yin HM. Simulation and experimental validation of heat

transfer in a novel hybrid solar panel. *International Journal of Heat and Mass Transfer*. Vol.55, 2012, pp.1076-1082.

[15] Popescu MC, Mastorakis N. Aspects regarding the use of renewable energy in EU country. *WSEAS Transactions on Environment and Development*, Vol. 6, No.4, 2010, pp. 265-275.

[16] Yang T, Athienitis AK. A study of design options for a building integrated photovoltaic/ thermal (BIPV/T) system with glazed air collector and multiple inlets. Solar Energy, 2014. DOI: 10.1016/j.solener.2014.01.049

[17] Kong XQ, Zhang D, Li Y, Yang QM. Thermal performance analysis of a direct-expansion solar-assisted heat pump water heater. *Energy*, Vol. 36, 2011, pp. 6830-6838.

[18] Wang Q, Liu Y, Liang G, Li J, Sun S, Chen G. Development and experimental validation of a novel indirect-expansion solar-assisted multifunctional heat pump. *Energy and Buildings*, Vol.43, 2011, pp. 300-304.

[19] Wang X, Zheng M, Zhang W, Yang T. Experimental study of a solar-assisted ground-coupled heat pump system with solar seasonal thermal storage in severe cold areas. *Energy and Buildings*, Vol.42, 2010, pp. 2104-2110.

[20] Ibrahim M, Sopian K, Daus WRW, Alghoul MA, Yaha M, Sulaiman MY, Zaharim A. Solar Chemical Heat Pump Drying System for Tropical Region. *WSEAS Tranactions on Environment and Development*, Vol.5, No.5, 2009, pp.404-413.

[21] Liu K., Ji J., Chow TT, Pei G., He H., Jiang A., Yang J. 2009. Performance study of a photovoltaic solar assisted heat pump with variable frequency compressor. A case study in Tibet. *Renewable Energy*. Vol. 32(12), pp. 2680-2687.

[22] Ozgener O., Hepbasli A. 2007. A review on the energy and exergy analysis of solar assisted heat pump systems. *Renewable and Sustainable Energy Reviews*, Vol. 11, pp. 482-496.

[23] Rossi C. Micro cogeneration from renewable energy system by means of innovative techniques for hybrid solar panels. PhD Thesis, 2013, DIME/TEC, University of Genoa.

[24] Rossi C., Tagliafico LA, Scarpa F., Bianco V. Experimental and numerical results from hybrid retrofitted photovoltaic panels. *Energy Conversion and Management*, Vol.76, 2013, pp. 634-644.

[25] Ji J., Pei G., Chow TT, Liu K., Han C. Experimental study of photovoltaic solar assisted heat pump system. *Solar Energy*. Vol. 82, No.1, 2008, pp. 43-52.

[26] Klein S.A. , Beckman W.A., Duffie J.A. A design procedure for solar heating systems. *Solar Energy*, Vol. 18, No. 2, 1976, pp. 113-127.